Available online at www.sciencedirect.com
ScienceDirect
International Communications in Heat and Mass Transfer 33 (2006) 1130 – 1138
International Communications in HEAT and MASS TRANSFER
www.elsevier.com/locate/ichmt

The recycle-effect on cool–thermal discharge systems under melt removal and flow rate variations ☆

C.D. Ho *, K.J. Hwang, J.W. Tu, Y.S. Su

Department of Chemical and Materials Engineering, Tamkang University, Tamsui, Taipei, Taiwan 251, ROC

Available online 12 July 2006

Abstract

A mathematical model to simulate the production of chilled air during on-peak power consumption hours in cool–thermal discharge systems with external recycle under melt removal and varied flow rate of flowing air has been developed theoretically. Equations have been derived for estimating the controlling air flow rate when the outlet chilled air temperature is specified. Three cases of inlet ambient temperatures of flowing air were illustrated to study the influence of recycle ratio on the performance improvement of cool–thermal discharge systems, the volumetric flow rate variations and Nusselt number increment due to a larger convective heat transfer rate were also delineated.

Keywords: Cool–thermal discharge; Heat transfer; Outlet chilled air; External recycles

1. Introduction

The implementation of cool–thermal storage and discharge devices into an energy system can improve load management, and will help to match electric utility supply and demand patterns. The storage and discharge operations have attractive features over energy costs ranging from low-cost hydroelectric and nuclear power to expensive gas turbines due to making ice during nighttime peak and producing chilled air from melting ice during daytime peak to supply air-conditioning needs. Restated, utility companies offer a cheaper rate at excess capacities during off-peak hours (typically 9 pm–9 am) of ice making to encourage energy use, leading to making good economic sense by saving electricity expense of power generation facilities and avoiding the danger shutdown due to insufficient supply of electricity.

A number of experimental and theoretical studies have been made on the improvements of the electricity utility profitability and energy efficiency in the cool–thermal storage system [1–3]. The theoretical analysis on cool–thermal discharge systems of specified heat fluxes and convective boundary has been developed [4,5]. The problem of predicting the behavior of heat convection–conduction system is difficult due to the presence of a moving interface, and rigorous theories could not be widely studied with a moving boundary [6–10].

☆ Communicated by W.J. Minkowycz.

* Corresponding author.
E-mail address: cdho@mail.tku.edu.tw (C.D. Ho).

0735-1933/$ - see front matter
doi:10.1016/j.icheatmasstransfer.2006.06.012

Nomenclature

c	specific heat (kJ kg^{-1} K^{-1})
V	air flow rate (m^3 s^{-1})
k	thermal conductivity (kJ m^{-1} h^{-1} K^{-1})
Nu_m	average Nusselt number
q	heat flow rate to ice from air (W)
Q_m	latent heat of ice melting (kJ kg^{-1} K^{-1})
R	recycle ratio
Re	Reynolds number
t	time (h)
t_0	total operating time per day (h)
$\bar{v}$	average air velocity (m h^{-1})
x	x-axis (m)
α_i	thermal diffusivity of ice (m^2 h^{-1})
μ_f	air viscosity (N s m^{-2})
ρ	density (kg m^{-3})
Subscripts	
f	air
i	ice

The applications of the recycle-effect concept in separation processes and reactor designs [11–13] with the desirable effect of the forced-convection increment are widely used in absorption, fermentation and polymerization while a maximum temperature strategy on the free surface to reduce the thermal resistance with melt removal is used in heat transfer problems [14]. Theoretical results show that the heat transfer efficiency improvement by increasing the recycle ratio in the devices with external recycle, and by removing the melt completely on the free surface may be achieved.

The merit of this new model is to present the positive influences of external recycle on the heat transfer rate enhancement and melt removal on the temperature gradient maximization between the free ice surface and flowing air in designing and operating the cool–thermal discharge systems. In our mathematical method, a study of flow rate variations of flowing air in situ contact cool–thermal discharges has been investigated to adjust the desired outlet air temperature for the practical demand in our daily life. The device performance of three inlet ambient air temperature is also illustrated with the recycle ratio and specified outlet air temperature as parameters.

2. Mathematical formulation

Fig. 1 shows the working dimension for the cool–thermal discharge system of length L, width B and thickness W ($\ll L$). The ambient air flows through the free ice surface and insulated plate, and will premix the recycle air RV of outlet temperature $T_{f,o}$ before entering the flow channel. The air flow rate is regulated by means of convectional pump placed at the end of the flow channel.

2.1. Before melting, $0 \le t \le t_i$

The initial temperature, T_∞, of the semi-infinite ice layer is kept uniform and below the melting point. Therefore, the ice layer starts melting until the surface temperature of the ice layer reaches the melting point, T_p, and the time for this moment is defined as t_i. Before melting, the heat transfer equation in ice layer is

$$\partial T/\partial t = \alpha_i(\partial^2 T/\partial x^2), \qquad 0 \le x \le \delta(t) \tag{1}$$

and the corresponding initial and boundary conditions are as follows:

$$\delta = 0 \text{ at } t = 0 \tag{2}$$

$$-k_i\left(\frac{\partial T}{\partial x}\right) = h_m(T_{f,m}-T) \text{ at } x = 0 \tag{3}$$

$$T(x,t) = T_\infty, \text{ at } x = \delta(t) \tag{4}$$

$$\frac{\partial T}{\partial x} = 0, \text{ at } x = \delta(t) \tag{5}$$

where h_m is the average heat convection coefficient of flowing air and $T_{f,m}=(T^*_{f,i}+T_{f,o})/2$ denotes the arithmetic–mean temperature in which $T^*_{f,i}=(T_{f,i}+RT_{f,o})/(1+R)$ refers the mixed inlet air temperature. The temperature distribution of ice layer before melting is obtained by using the approximation method of integral boundary–layer analysis [4,8] with assuming a quadratic form of temperature distribution in ice layer as follows:

$$T = \frac{\delta(t)h_m}{2k_i + \delta(t)h_m}(T_{f,m}-T_\infty)\left(\frac{x}{\delta(t)}-1\right)^2+T_\infty \tag{6}$$

For the case of forced-convection flow between two parallel plates with one side heated and the other side insulated in cool–thermal discharge systems, the average heat transfer coefficient in Eq. (8) was derived by the empirical equation [15] for turbulent flow

$$h_m = 0.0158\frac{k_f \cdot \mathrm{Re}^{0.8}}{D_e}, \ \mathrm{Re} > 2100 \tag{7}$$

in which $Re=D_e(1+R)V\rho_f/\mu_f BW$ is the Reynolds number of the flowing air. Furthermore, the thermal penetration distance when $t=t_i$ can be determined by Eq. (8) as

$$\delta(t_i) = \delta_0 = \frac{-2k_iT_\infty}{h_mT_{f,m}} \tag{8}$$

2.2. After melting, $t \geq t_i$

The water layer starts forming while the temperature at free ice surface reaches the melting point. In order to decrease the thermal resistance between the hot air and ice layer, the water layer is removed immediately and

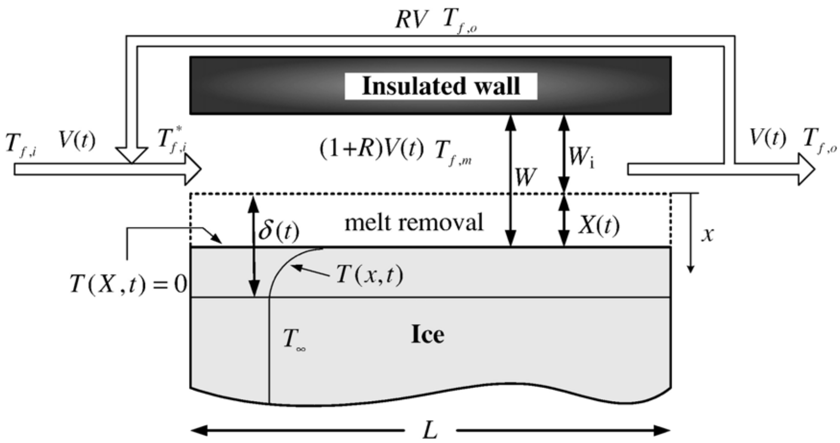

Fig. 1. Schematic diagram of cool–thermal discharge systems under melt removal.

completely. The corresponding governing equation and initial and boundary conditions after melting are

$$\partial T/\partial t = \alpha_i(\partial^2 T/\partial x^2), \qquad X(t) \leq x \leq \delta(t) \tag{9}$$

$$X(t) = 0 \text{ at } t = t_i \tag{10}$$

$$T = T_p \text{ at } x = X(t) \tag{11}$$

$$h_m\left[T_{f,m} - T_p\right] = \rho_i Q_m \frac{\mathrm{d}X}{\mathrm{d}t} + \left[-k_i\left(\frac{\partial T}{\partial x}\right)\right] \text{ at } x = X(t) \tag{12}$$

$$T = T_\infty \text{ at } x = \delta(t) \tag{13}$$

$$\frac{\partial T}{\partial x} = 0 \text{ at } x = \delta(t) \tag{14}$$

where $X(t)$ is the ice melting thickness. One obtains the solution of the temperature distribution as the same procedure performed in the previous section

$$T(x,t) = 2T_\infty\left(\frac{x(t) - X(t)}{\delta(t) - X(t)}\right) - T_\infty\left(\frac{x(t) - X(t)}{\delta(t) - X(t)}\right)^2 \tag{15}$$

Hence, the ice melting thickness $X(t)$ and thermal penetration thickness $\delta(t)$ were solved numerically from Eqs. (16) and (17), and thus, the temperature distribution in ice layer was calculated from Eq. (15).

$$\frac{\mathrm{d}X(t)}{\mathrm{d}t} = \frac{1}{\rho_i Q_m}\left(h_m T_{f,m} + \frac{2k_i T_\infty}{\delta(t) - X(t)}\right) \tag{16}$$

and

$$\frac{\mathrm{d}\delta(t)}{\mathrm{d}t} = \frac{-6Q_m\alpha_i\rho_i + 4k_i T_\infty + 2h_m[\delta(t) - X(t)]T_{f,m}}{Q_m[X(t) - \delta(t)]\rho_i} \qquad t \geq t_i \tag{17}$$

3. Average Nusselt number and heat transfer efficiency improvement

By assuming the heat flux transferred to raise the temperature in ice layer as sensible heat is negligible, the heat discharging rate from the ambient air to the ice layer on free surface may be expressed in terms of the arithmetic mean temperature of the air $T_{f,m}$

$$q(t) = BLh_m[T_{f,m} - T(0,t)] = V\rho_f c_f(T_{f,i} - T_{f,o}) \tag{18}$$

Therefore, the outlet temperature $T_{f,o}$ and arithmetic mean temperature of the air $T_{f,m}$ can be presented in the form of Eqs. (19) and (20), respectively

$$T_{f,o} = \frac{[2(1+R)V\rho_f c_f - h_m BL]T_{f,i} + 2(1+R)h_m BLT(0,t)}{2(1+R)V\rho_f c_f + (1+2R)h_m BL} \tag{19}$$

$$T_{f,m} = \frac{2(1+R)V\rho_f c_f T_{f,i} + (1+2R)h_m BLT(0,t)}{2(1+R)V\rho_f c_f + (1+2R)h_m BL} \tag{20}$$

The Nusselt number provides a measure of the convection heat transfer occurring at the surface as

$$\mathrm{Nu}_m = \frac{h_m D_e}{k_f} \tag{21}$$

in which $D_e=2W=2[W_i+X(t)]$ denotes the equivalent diameter of the air flowing passage, and the average heat convection coefficient of flowing air can be derived from Eq. (22)

$$h_m = \frac{V\rho_f c_f (T_{f,i} - T_{f,o})}{BL[T_{f,m} - T(0,t)]} \tag{22}$$

Then the Nusselt number can be rewritten as follows:

$$\mathrm{Nu}_m = \frac{2WV\rho_f c_f (T_{f,i} - T_{f,o})}{BLk_f[T_{f,m} - T(0,t)]} \tag{23}$$

where the outlet temperature $T_{f,o}$ and arithmetic mean temperature $T_{f,m}$ of the air were calculated from Eqs. (19) and (20). The heat transfer improvement of a cool–thermal discharge system with recyclic operation is defined by calculating the percentage increase in heat transfer rate based on that of a single-pass device with the same working dimension and operating conditions

$$I_h = \frac{(\mathrm{Nu}_m)_R - (\mathrm{Nu}_m)_{R=0}}{(\mathrm{Nu}_m)_{R=0}} \tag{24}$$

4. Hydraulic dissipated power increment

The recyclic operation increases not only the convective heat transfer coefficient of flowing air but also the friction loss on the insulate wall and ice surface. The power consumption in the conduit may be estimated by

$$P = (R+1)V\rho_f \ell w_f = \frac{[(R+1)V]^2 fL\rho_f}{g_c BW^2} \tag{25}$$

where $\ell wf=2fVL/(g_cBW^2)$ denotes the friction loss in the conduit. The Blasius equation, $f=0.079\ Re^{-025}$, was used to determine the friction loss in the conduit for the Reynolds number of fluid, Re, below 100,000 in the turbulent flow. The power consumption increment I_p due to the recyclic operation was illustrated to calculate the percentage increase compared to a single-pass device as follows:

$$I_p(t) = \frac{P(t) - P_{R=0}(t)}{P_{R=0}(t)} = \left[(R+1)^{2.75} \cdot \left(\frac{W_{R=0}}{W}\right)^{0.25}\right] - 1 \tag{26}$$

Some results of I_p after 10-h operation for three cases are shown in Table 1.

Table 1
The power consumption increment of three cases after10-h operation with $T_{f,o}$ and recycle ratio as parameters

I_P	$T_{f,o}$=298 K		$T_{f,o}$=297 K		$T_{f,o}$=296 K	
	R=1	R=2	R=1	R=2	R=1	R=2
Case 1	4.60	12.96	8.13	21.38	20.45	52.36
Case 2	5.24	16.70	12.68	35.23	48.61	129.45
Case 3	8.30	19.85	25.46	71.23	93.14	266.95

5. Numerical examples

The air outlet temperature was specified with the operating time t_0 of the discharge period in one day. The heat transfer efficiency improvement by employing the recycle device was illustrated by the following three desired air outlet temperatures, $T_{f,o}$=296 K, 297 K and 298 K with three cases of inlet ambient temperatures

$$\text{Case 1}-\ T^1_{f,i} = 305\ \text{K (constant)}, \tag{27}$$

$$\text{Case 2}-\ T^2_{f,i} = 304\ \text{K} + 2\ \sin(\pi t/t_0), \tag{28}$$

$$\text{Case 3}-\ T^3_{f,i} = 303\ \text{K} + 5\ \sin(\pi t/t_0). \tag{29}$$

The working dimensions of the recyclic device are L=10 m, B=4 m and W_i=0.1 m with the operating conditions T_p=273 K, T_∞=253 K, p=1 *atm* and t_0=10 h, and the physical properties of ice and air are given [16,17]. The theoretical predictions of the air volumetric flow rate and average Nusselt numbers are obtained and represented in Figs. 2–4.

6. Results and discussions

The calculation procedure is described briefly as follows. First, the initial air volumetric flow rate can be determined by combining Eqs. (7) and (19) for a specified outlet temperature. Second, combining Eqs. (7) and (22) and differentiating the resultant equation, one can obtain the differential equation of air volumetric flow rate as

$$\mathrm{d}V/\mathrm{d}t = f(\delta'(t), \delta(t), V(t)) \tag{30}$$

in which, $\delta'(t)$ can be obtained by substituting Eq. (6) into Eq. (1) and integrating Eq. (1) with respect to x with the aid of the boundary conditions, say Eqs. (3) and (5). Therefore, the air volumetric flow rate, $V(t)$, and the thermal penetration distance, $\delta(t)$, before melting can be obtained by solving the $V'(t)$ and $\delta'(t)$ simultaneously. Furthermore, the ice melting thickness, $X(t)$, $\delta(t)$ and $V(t)$ after melting can be determined by solving Eqs. (16), (17) and (30) simultaneously.

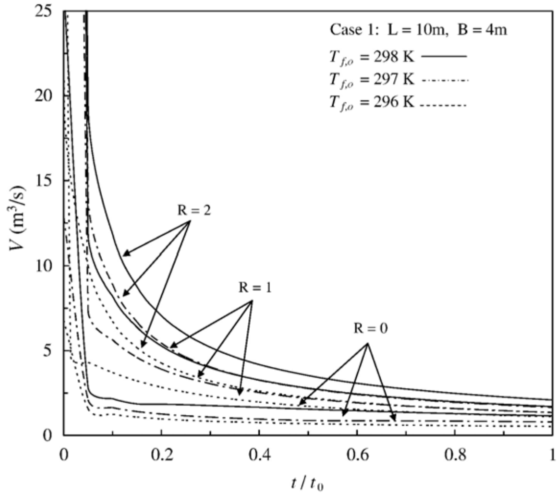

Fig. 2. Time history of air flow rate with recycle ratio as a parameter for Case 1.

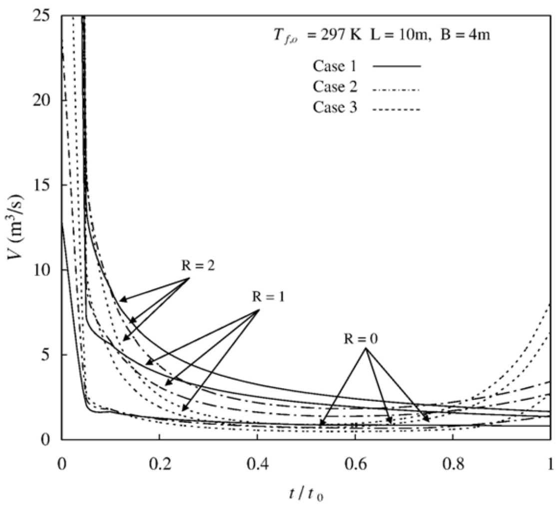

Fig. 3. Time history of air flow rate with recycle ratio as a parameter for three cases.

Fig. 2 shows the time history of air flow rate with recycle ratio as a parameter for Case 1. The air flow rate decreases with operating time due to the channel thickness expanded as the ice melting proceed with operating time, as shown in Fig. 2. It is seen from Fig. 2 that the air flow rate also increases with increasing recycle ratio for three fixed outlet temperature cases. The production increment of chilled air in a cool–thermal discharge system was achieved with external recycle, as confirmed by Fig. 2. The time histories of air flow rate for three inlet ambient temperatures with the given outlet temperature $T_{f,o}$=297 K are shown in Fig. 3. Case 1 represents the constant ambient temperature during the whole operating time while Cases 2 and 3 show the practical system of ambient temperature varied with time from sunrise to sunset. Because of the inlet air temperature varies during operation processes in Cases 2 and 3, the air flow rate varies with operating time as well. It is shown in Fig. 3 that the air flow rate increases with increasing with recycle ratio for three inlet ambient temperatures.

The application of recycle-effect concept to the cool–thermal discharge systems creates two conflict effects on the heat transfer rate. The advantage effect is the convective heat transfer coefficient enlargement due to the air flow rate increment in the conduit while the disadvantage effect is the decreasing of the temperature driving force between the flowing air and free ice layer surface owing to premixing the fresh ambient air by the recycle air $RV$of outlet temperature

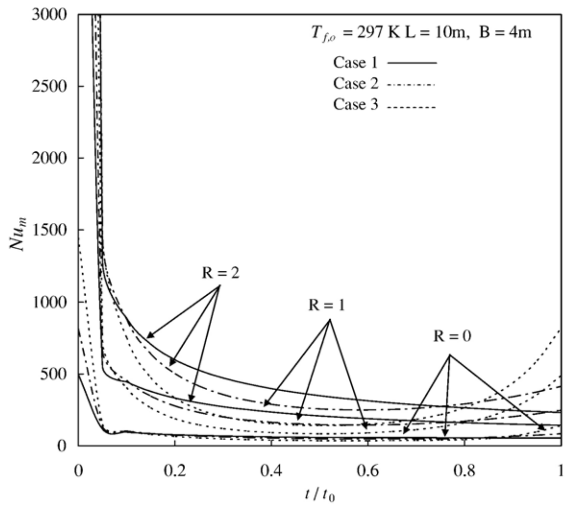

Fig. 4. Time history of the average Nusselt number with recycle ratio as a parameter for three cases.

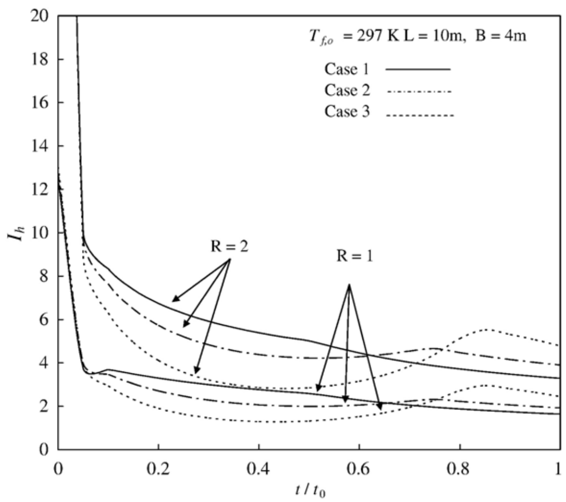

Fig. 5. Time history of I_h with recycle ratio as a parameter for three cases.

$T_{f,o}$ before entering the flow channel. The theoretical results show that the advantage effect overcomes the disadvantage one and leads to an improved device performance.

Nusselt number is usually determined as a measurement of the convection heat transfer occurring at the surface in a heat transfer problem. The average Nusselt number was computed by Eq. (23) and illustrated in Fig. 4. Fig. 4 shows that the average Nusselt number increases with increasing recycle ratio for all three practical cases. Moreover, the heat transfer efficiency improvement of a cool–thermal discharge system with external recycle was calculated by Eq. (24) based on the system without external recycle. The heat transfer efficiency improvement increases with increasing recycle ratio for the three cases, as indicated from Fig. 5. Besides, the power consumption increment due to the recyclic operation was calculated by Eq. (26). The power consumption increment after 10-h operation for three cases increases with increasing the recycle ratio and outlet air temperature, as observed from Table 1.

7. Conclusions

A theoretical analysis of a cool–thermal discharge system with external recycle has investigated in the present study. The required air flow rate for producing the specified temperature outlet chilled air was estimated by making the energy balance with integral boundary–layer analysis on the free surface. Three practical inlet ambient temperatures were taken as the numerical examples with three desired outlet air temperature, say $T_{f,o}$=296 K, 297 K and 298 K, as parameters. The theoretical predictions show that the air flow rate for producing the specified temperature outlet chilled air increases with recycle ratio and outlet air temperature as the discharging process proceeds during 10-h operation. As the same trends of the required air flow rate, the average Nusselt number increases with recycle ratio and changes sensitively with the operating time. Accordingly, the heat transfer efficiency improvement by employing the device with external recycle in cool–thermal discharge systems was determined by Eq. (24). The heat transfer efficiency improvement increases with increasing recycle ratio as indicated in Fig. 5. It is concluded that the recyclic operation can readily improve the heat transfer efficiency of a cool–thermal discharge system, and the more amount of chilled outlet air was produced with increasing the recycle ratio for a specified desired outlet chilled air temperature.

References

[1] D.H. Hersh, DDC and ice thermal storage systems provide comfort and energy efficiency, ASHRAE J. 36 (3) (1994) 35–37.

[2] C.E. Dorgan, J.S. Elleson, ASHRAE's new design guide for cool thermal storage, ASHRAE J. 36 (5) (1994) 29–34.

[3] H.M. Yeh, C.Y. Cheng, Cool thermal storage by vacuum freezing of water, Energy 16 (1991) 1045–1049.

[4] C.D. Ho, H.M. Yeh, Y.S. Su, Improvement in performance of cool–thermal discharge systems from ice melting with producing chilled air under constant heat flux and external refluxes, Numer. Heat Transf., A Appl. 45 (2004) 505–516.

[5] C.D. Ho, A theoretical study of the recycle effect on heat transfer efficiency in cool–thermal discharge systems from ice melting with producing chilled air, Numer. Heat Transf., A Appl. 46 (2004) 277–299.
[6] S.S. Penner, S. Sherman, Heat flow through composite cylinders, J. Chem. Phys. 15 (1947) 569–574.
[7] L. Roberts, On the melting of a semi-infinite body of ice placed in a hot stream of air, J. Fluid Mech. 4 (1958) 505–528.
[8] T.R. Goodman, B. Mass, The heat-balance integral and its application to problems involving a change of phase, Trans. ASME 8 (1958) 335–342.
[9] H.S. Carslaw, J.C. Jaeger, Conduction of Heat in Solidssecond ed., Oxford Univ. Press, New York, 1959.
[10] E.R.G. Eckert, R.M. Drake Jr., Analysis of Heat and Mass Transfer, McGraw-Hill, New York, 1972.
[11] R. Marquart, H. Blenke, Circulation of moderately to highly viscous Newtonian and non-Newtonian liquids in propeller pumped circulating loop reactors, Int. Chem. Eng. 20 (1980) 368–378.
[12] R. Franciso, W.L. Luyben, Extensions of the simultaneous design of gas-phase adiabatic tubular reactor systems with gas recycle, Ind. Eng. Chem. Res. 40 (2001) 635–647.
[13] A.G. Jones, Liquid circulation in a drift-tube bubble column, Chem. Eng. Sci. 40 (1985) 449–462.
[14] C.D. Ho, H.M. Yeh, W.P. Wang, J.K. Wang, Cool thermal discharge obtained with air flowing over melting ice by complete removal of melt, Int. Commun. Heat Mass Transf. 27 (2000) 785–794.
[15] W.M. Kays, M.E. Crawford, Convective Heat and Mass Transfer, McGraw-Hill, New York, 1980.
[16] D.P.D. Incropera, Fundamentals of Heat and Mass Transfer, 3rd ed.John and Sons, New York, 1990.
[17] C.J. Geankoplis, Transport Processes and Unit Operations, Allyn and Bacon Inc., Boston, 1983.